Autophosphorylation is a mechanism of inhibition in twitchin kinase

Rhys M. Williams[1,2], Barbara Franke[1,2], Mark Wilkinson[2], Jennifer R. Fleming[1], Daniel J. Rigden[2], Guy M. Benian[3], Patrick A. Eyers[2], Olga Mayans[1,2]

[1]Department of Biology, University of Konstanz, 78457 Konstanz, Germany; [2]Department of Biochemistry, Institute of Integrative Biology, University of Liverpool, Crown Street, Liverpool, L69 7ZB, UK; [3]Department of Pathology, Emory University, Atlanta, GA 30322, USA.

To whom correspondence should be addressed:
Prof. Olga Mayans, Tel: +49-7531 882212, olga.mayans@uni-konstanz.de

Running Title: Autophosphorylation of twitchin kinase

Abstract

Titin-like kinases are muscle-specific kinases that regulate mechanical sensing in the sarcomere. Twitchin kinase (TwcK) is the best-characterized member of this family, both structurally and enzymatically. TwcK activity is auto-inhibited by a dual intrasteric mechanism, in which N- and C-terminal tail extensions wrap around the kinase domain, blocking the hinge region, the ATP binding pocket and the peptide substrate binding groove. Physiologically, kinase activation is thought to occur by a stretch-induced displacement of the inhibitory tails from the kinase domain. Here, we now show that TwcK inhibits its catalysis even in the absence of regulatory tails, by undergoing auto-phosphorylation at mechanistically important elements of the kinase fold. Using mass spectrometry, site-directed mutagenesis and catalytic assays on recombinant samples we identify residues T212, T301, T316 and T401 as primary auto-phosphorylation sites in TwcK *in vitro*. Taken together, our results suggest that residue T316, located in the peptide substrate binding P+1 loop, is the dominantly regulatory site in TwcK. Based on these findings, we conclude that TwcK is regulated through a triple inhibitory mechanism consisting of phosphorylation as well as intrasteric blockage, which is responsive not only to mechanical cues but also to biochemical modulation. This implies that mechanically stretched conformations of TwcK do not necessarily correspond to catalytically active states, as previously postulated. This further suggests a phosphorylation-dependent desensitization of the TwcK-mediated mechanoresponse of the sarcomere *in vivo*.

Keywords

Kinase regulation / mass spectrometry / site-directed mutagenesis / phosphotransfer catalysis

Introduction

The giant proteins of the titin family are integral components of the muscle sarcomere, where they play crucial roles in development, structure, regulation and mechanics (1,2). Members of the titin family include titin and obscurin in mammals; twitchin/UNC-22, the obscurin homolog UNC-89 and TTN-1 in nematodes; twitchin in molluscs; projectin, UNC-89 and stretchin in insects (3,4). These proteins share related architectures. They consist of large, filamentous polypeptide chains (0.7-4 MDa) that fold into numerous immunoglobulin (Ig) and fibronectin type III (FnIII) domains linked in tandem, several unique sequences and one or two kinase domains that are located near their C-terminus. The kinase domain and its immediate flanking domains are highly conserved across members of this family, but specific variations in active site features have led to the suggestion that some members of the family, such as UNC-89-PK1 (5) and titin kinase (6), are actually pseudokinases. Both canonical and pseudokinase members of this family recruit to the sarcomere protein factors associated with muscle turn-over or stress response, e.g. Nbr1/p62/MuRF2, MuRF1, and MAPKAP kinase 2 (5-8). This suggests that titin-like kinases might be functionally involved in muscle remodelling or stress response.

Twitchin kinase (TwcK) from *C. elegans* is the best-studied member of the titin kinase family, having been characterized structurally (9-11) and enzymatically (6,11-13). Crystal structures of TwcK show that the kinase domain is regulated intrasterically by N- and C-terminal extensions that pack against mechanistically important regions of the fold to modulate catalytic activity. The N-terminal linker (NL) extension wraps around the N-terminal lobe of the kinase domain, occupying much of the interlobular hinge region. The C-terminal regulatory extension (CRD) packs directly onto the active site, blocking the access of ATP and peptidic substrates to their respective binding sites. Both NL and CRD extensions have been shown to be inhibitory, with the isolated kinase domain of TwcK (lacking both regulatory tails) displaying the highest levels of catalysis *in vitro* (11). The crystal structure of human titin kinase (TK) (6,14) and TwcK from *Aplysia* (10) revealed the presence of highly similar CRD extensions, which together with sequence analyses of numerous other titin-like kinases (5,11) suggests that the dual instrateric inhibition observed in *C. elegans* TwcK might be a conserved mechanism in this kinase family.

To date, no protein activator has been identified that can release the catalytic inhibition exerted by NL and/or CRD tails in any titin-like kinase. Instead, it is thought that these kinases might be activated mechanically, with the tails being displaced from the kinase core by stretch-unfolding as a result of the pulling forces that develop in the sarcoskeleton in the active muscle (11,15-17). More recently, TwcK has been found to be a substrate of MAPKAP kinase 2, a stress-activated kinase that appears to bind to the CRD tail of TwcK (8). However, it is yet to be established whether phosphorylation by MAPKAP kinase 2 can alter tail packing in TwcK and result in its activation.

In contrast to the increasing knowledge of their intrasteric regulation, little is known about autocatalytic mechanisms in titin-like kinases, namely their possible regulation by auto-phosphorylation. Early reports suggested that TwcK from *Aplysia* (18) and from *C. elegans* (12) undergo auto-phosphorylation, but no further studies emerged from those works. Building upon those early observations, we have now investigated the capability of TwcK to regulate its phosphotransfer catalysis through auto-phosphorylation within the kinase domain *in vitro*. Our findings indicate that TwcK auto-phosphorylates several mechanistically-relevant amino acids which then inhibit catalysis. This constitutes a new regulatory mechanism for TwcK in which catalytic silencing is possible even in the absence of intrasteric inhibition by the NL and CRD tails. We discuss the possible implications of these findings for the phosphorylation-dependent mechano-enzymatic response of TwcK in the sarcomere.

Methods

Cloning and site-directed mutagenesis

The expression plasmid of *C. elegans* TwcK (UniProtKB Q23551; residues 6108-6685) has been previously reported (11). To simplify annotation and aid the visual mapping of residues mentioned in this work, we have adopted the residue numbering used in PDB entry 3UTO, taking residue 6108 to be residue 1. All TwcK constructs used here were ligated into the pETM-11 vector via NcoI and KpnI restriction sites. This

yielded a protein product containing a His_6-tag and a TEV protease cleavage site fused N-terminally to the TwcK variant under study.

Mutagenesis was performed by whole plasmid PCR amplification with Q5 DNA polymerase (NEB) using back-to-back primers containing the desired mutation in the forward primer only. Mutations were confirmed by complete sequencing of the coding region (Source BioScience).

Recombinant protein production

All protein samples were expressed in *E. coli* Rosetta cells (Merck Millipore). Cultures were grown in LB media supplemented with 25 µg/mL kanamycin and 34 µg/mL chloramphenicol at 37°C to an OD_{600} of 0.6-0.8. Protein expression was induced by addition of 0.5 mM isopropyl β-D-1-thiogalactopyranoside followed by growth at 18°C for approx. 18 hrs. Cell pellets were harvested by centrifugation in 50 mM Tris-HCl pH 7.9, 500 mM NaCl, 1 mM dithiothreitol (lysis buffer) in the presence of 20 µg/mL DNase I (Sigma Aldrich) and an EDTA-free complete protease inhibitor cocktail (Roche). Cell lysis was by sonication followed by clarification of the lysate by centrifugation for 45 min at 39,000g. The lysate was applied to Ni^{2+}-NTA resin (Qiagen) equilibrated in lysis buffer containing 20 mM imidazole. Elution used 200 mM imidazole. Removal of imidazole from eluted samples was by buffer exchange into lysis buffer using PD-10 columns (GE Healthcare). His_6-tag removal by TEV protease cleavage was carried out overnight at 4°C, followed by subtractive Ni^{2+}-NTA purification. Gel filtration was performed on a Superdex 200 16/60 column (GE Healthcare) in 50 mM Tris-HCl pH 7.9, 50 mM NaCl, 1 mM dithiothreitol. The purified samples were stored at 4°C until further analysis.

[γ^{32}P]-ATP phosphotransfer assays

To measure the catalytic activity of TwcK, phosphotransfer assays were performed using 30 ng of TwcK in a 40 µL reaction volume. An established peptide model substrate derived from chicken myosin light chain (kMLC11-23) with the sequence KKRARAATSNVFS was employed (11,13). Each reaction contained 20 mM

Tris-HCl pH 7.4, 10 mM $MgCl_2$, 0.2 mg/mL BSA, 0.2 mg/mL peptide substrate and 200 μM [γ^{32}P]-ATP (~2 μCi per reaction). Samples were incubated at 25^{o}C for 20 minutes and reactions halted by blotting 38 μL onto P81 phosphocellulose paper, prior to rapid immersion in 100 mM phosphoric acid, followed by triplicate 100 mM phosphoric acid washes for 5 minutes per wash. Papers were then immersed in acetone and air-dried. Control reactions contained peptide substrate without kinase and kinase alone without peptide substrate. Quantification of samples and calculation of ATP activity was performed by Cerenkov counting (19) using a Beckman Coulter scintillation counter. Activities were quantified in nmol phosphate by calculating the specific activity of 1 nmole of ATP from counts obtained for 2 μL of 1 mM [γ^{32}P]-ATP (~0.25 μCi) spotted directly onto P81 phosphocellulose paper and counted.

Dephosphorylation of twitchin kinase by lambda phosphatase

Purified TwcK (approx. 8 μg) was incubated at 25^{o}C with 100 U of lambda phosphatase (NEB) in 50 mM HEPES pH 7.5, 10 mM NaCl, 2 mM dithiothreitol, 0.01% Brij 35 supplemented with 1 mM $MnCl_2$. After 1 hour, the reaction was halted by boiling with SDS-PAGE loading buffer (30 mM Tris-HCl pH 6.8, 12.5% [v/v] glycerol, 1% [w/v] SDS, 35 mM β-mercaptoethanol) followed by analysis using SDS-PAGE.

For TwcK dephosphorylation prior to phosphotransfer assays, Ni^{2+}-NTA purified TwcK (approx. 5 mg) was incubated with 400 units of lambda phosphatase in 50 mM Tris-HCl pH 7.9, 500 mM NaCl, 1 mM dithiothreitol, 1 mM $MnCl_2$ for 1 hour at room temperature followed by overnight incubation at 4^{o}C. Lambda phosphatase was then separated from TwcK by an additional Ni^{2+}-NTA purification step followed by His_6-tag removal by TEV protease and further purification by gel filtration as described above.

Mass spectrometry

To obtain an intact mass of the recombinant TwcK product, desalted TwcK was infused into the nano-electrospray source of a Waters Q-ToF micromass spectrometer at a flow rate of 50 μl/hour via a gas tight syringe. The positive ion mass spectrum of the sample was scanned in the range m/z 80 to 2,000 using a scan time of 1 second and a data

acquisition time of 5 minutes. MassLynx MaxEnt1 was then used to convert the summed multiply charged spectrum to a molecular mass spectrum.

In preparation for phosphorylation site identification, TwcK and its variants were digested in solution overnight in 25 mM Tris-HCl, 2 M urea, pH 7.8 using trypsin, Lys-C and Glu-C; either individually or in various protease combinations. MALDI-MS analysis was performed using a MALDI-Tof instrument (Waters-Micromass) on digests that had been enriched for phosphopeptides using either titanium oxide or Fe^{3+}-IMAC mini columns. Peptide mixtures were analysed using a saturated solution of alpha-cyano-4 hydroxycinnamic acid in 50% acetonitrile/0.1% trifluoroacetic acid. Peptides were selected in the mass range of 1000 – 4000 Da. For ES-MS, the digests were desalted with C18 Zip Tips (Merck Millipore) and analysed as described above for intact TwcK. Several individual peptides were subjected to ES-MS/MS for sequence analysis.

In-gel trypsin digests were also performed on TwcK samples after fractionation by SDS-PAGE. Following an overnight incubation, the peptides were extracted from the gel pieces, desalted using C18 Zip Tips and analysed by MALDI-MS as described above.

Computational exploration of TwcK phosphorylation sites

FoldX BuildModel (20) was used to introduce mutations and phosphoryl groups *in silico* using the crystal structure of TwcK kinase domain, which was extracted from PDB 3UTO (by deletion of regulatory tails and additional flanking domains). FoldX Repair (20) was then used for energy minimisation of wild-type and phosphorylated structures.

For molecular dynamic simulations (MDS), the phosphorylated form of residues T301 and T316 (pT301 and pT316, respectively) were modeled using the Vienna-PTM 2.0 server (21). The models were placed in the center of a rhombic dodecahedron water box (at 1.0 nm from the box edge) and counterions added to the system (Na^+, Cl^- at a concentration of 50 mM). Simulations were performed using GROMACS package 5.0 (22) with the AMBER99SB-ILDN forcefield (23). The SPC-E water model was used. An initial energy minimization of all systems was performed using the steepest descent algorithm. The Particle Mesh Ewald (PME) algorithm (24) was used for long-range electrostatics with non-bonded and van der Waals cut-offs of 1nm. All bond lengths were constrained using the LINCS algorithm (25). Calculations used a constant temperature of

300K, a pressure of 1 bar, an integration time step of 2 fs with periodic boundary conditions. A final MD run of 100 ns was performed for all systems. Structures were analyzed using tools available in GROMACS: gmx rmsf (22).

Results

Twitchin kinase undergoes auto-phosphorylation

TwcK samples that had been expressed recombinantly in *E. coli* and purified by column chromatography displayed significant heterogeneity. The samples migrated as multiple species in SDS-PAGE, with three major states exhibiting apparent molecular masses between ~32 and ~35 kDa (**Fig 1a**). Protein identification using tryptic-digestion followed by mass spectrometry (MS) confirmed all SDS-PAGE bands to be composed of TwcK. Treatment of TwcK samples with lambda phosphatase led to the collapse of all migrating bands onto a single species of lowest apparent molecular weight (i.e. furthest migrating TwcK species in SDS-PAGE) (**Fig 1b**). Similarly, incubation of lambda phosphatase treated TwcK samples with ATP/Mg^{2+} led to re-phosphorylation as confirmed by intact mass determination using mass spectrometry (Supplementary **Fig S1**).

To further confirm that the observed modification of TwcK was due to auto-phosphorylation, we assayed a catalytically inactive TwcK variant carrying the mutation K185A in the active site ($TwcK^{K185A}$). Residue K185 (a lysine residue in β-strand β3) is highly conserved in the protein kinase superfamily (26,27). This lysine is essential for phosphotransfer due to its role in the coordination of ATP, which it chelates through an electrostatic interaction with the α- and β-phosphate groups. Recently, we established that $TwcK^{K185A}$ is catalytically inactive using phosphotransfer assays (28). In the current study, we observed that the inactive $TwcK^{K185A}$ migrates in SDS-PAGE as a single species of apparent molecular weight lower than any of the observable wild-type TwcK species, but equivalent to phosphatase-treated TwcK samples (**Fig 1b**). This observation further supports the conclusion that the multiple species of recombinantly expressed TwcK are the result of auto-phosphorylation.

Hyperphosphorylation is linked to TwcK inactivation

Phosphorylation is a well-established regulatory mechanism of protein kinases (reviewed in 26), and although it is most commonly associated with an enhanced catalytic output, phosphorylation of some kinases (e.g. GSK-3) can lead to their physiological inactivation (29). In order to analyze the effect of phosphorylation on TwcK catalysis, species migrating as 'upper' and 'lower' bands in SDS-PAGE, corresponding to different phosphorylation states, were partially separated using size exclusion chromatography (SEC) and compared side-by-side for phosphotransfer activity on a model peptide substrate (**Fig 1c).** Unexpectedly, the faster-migrating 'lower bands' corresponding to hypo-phosphorylated TwcK displayed notably elevated activity (172-188 nmol phosphate·min^{-1}·mg^{-1}). In contrast, the same quantity of protein from 'upper bands' that contain hyper-phosphorylated TwcK exhibited notably less activity (5-9 nmol phosphate·min^{-1}·mg^{-1}), corresponding to ~4% of the activity associated with the hypo-phosphorylated kinase. We questioned whether this low-level activity might actually arise from residual hypo-phosphorylated TwcK present in those fractions, since separation by SEC was not likely to be fully efficient. Accordingly, various additional chromatographic separation techniques, including anion exchange and Fe^{3+}-IMAC (Immobilized Metal Affinity Chromatography), were conducted in an attempt to improve the separation of differently phosphorylated TwcK species. However, all species co-eluted using these techniques and, in fact, SEC provided the best achievable separation. Thus, we concluded that the catalytic output of the hyper-phosphorylated TwcK might be actually lower than the measured activity assigned here.

Our deduction that hyper-phosphorylation inhibits TwcK catalysis was supported by experiments employing non-phosphorylated samples. TwcK that had been treated with lambda phosphatase showed enhanced activity towards the model peptide substrate, up to ~ 35% higher than that of the hypo-phosphorylated TwcK species (**Fig 1c**). The complete removal of phosphoryl groups by lambda phosphatase treatment of TwcK was confirmed by ES-MS intact mass determination, which showed that the measured mass matched that calculated from sequence data and, thereby, corresponded to unmodified TwcK **(Fig 2b)**. During catalysis, it can be expected that the phosphorylation of the peptide substrate must be happening concurrently with TwcK autophosphorylation. However, in the

phosphotransfer assay applied in this study, the peptide substrate is added to TwcK in substantially large excess (~8000 fold molar excess). Under such oversaturating conditions, substrate phosphorylation could be expected to be the dominant catalytic process, with the concurrent on-going autophosphorylation being sufficiently disfavoured as to yield the observed difference in catalysis. In summary, the measured TwcK phosphotransfer activity is highest in dephosphorylated or minimally-phosphorylated samples, while high levels of auto-phosphorylation are associated with low levels of catalytic activity (resulting in inhibition).

Identification of multiple auto-phosphorylation sites in TwcK by mass spectrometry

Intact mass analysis of TwcK samples by ES-MS confirmed the existence of multiple phosphorylation states, consistent with our SDS-PAGE analysis (**Fig 2a**). Three major masses (32756, 32836 and 32916 Da) were measured, each differing in the mass of a phosphoryl group (80 Da). The lowest value observed (32756 Da) is 162 Da larger than the mass measured lambda phosphatase-treated TwcK samples (32594 Da), corresponding to a species including two phosphorylated amino acids, indicating that non-phosphorylated or mono-phosphorylated TwcK species are of very low abundance in recombinant samples. Accordingly, the peaks at 32836 Da and 32916 Da corresponded to triple and quadruple phosphorylation states of TwcK. Smaller peaks at higher mass values were observed at intervals consistent with higher phosphorylated states in the sample population, pointing to the existence (at lower abundance) of up to six phosphorylation sites in TwcK in total.

To identify the phosphorylation sites responsible for these mass differences, TwcK isoforms were subjected to various forms of proteolytic fragmentation with subsequent MS analysis (**Fig 2c**). Digestion of TwcK using a combination of trypsin and Glu-C proteases, followed by enrichment of phosphopeptides and MALDI-MS analysis revealed that the masses for peptides S290-D305 and S290-K307 (the latter containing a missed trypsin cleavage) were increased by 80 Da and 160 Da with respect to their predicted masses, suggesting double phosphorylation within this sequence. S290 and T301 are the only phosphorylatable residues in this sequence, thus, both residues are likely subject to phosphorylation. Further direct evidence for T301 phosphorylation was

found with the observation of a peptide with the mass expected for a L295-K307 peptide with an additional mass of 80 Da. However, the phosphorylation of S290 was variably observed in several repetition experiments and we concluded that, likely, this is a secondary site of phosphorylation. In parallel, the phosphorylation of T212 was confirmed by the presence of a mass equivalent to that expected for peptide H210-E225 but increased by 80 Da, with the only phosphorylatable residue in this sequence being T212.

A further analysis was performed using digestion with trypsin and Lys-C proteases followed by ES-MS. Among the peptide masses observed were three distinct pairs of related peaks containing the expected mass for the non-phosphorylated peptide alongside that of the singly-phosphorylated peptide. We observed such pairs for the sequences M400-R419 [M+2H+ ion] containing residues T401 and T412; H210-K241 [M+3H+ ion] containing S234 and the previously identified T212 (which served as confirmation of this site); and T313-R363 [M+4H+ ion] containing T313, T314 and T316. In each of these peptides, only a single site was phosphorylated. Based on an evaluation of the TwcK crystal structure (PDB: 3UTO (11)), T316 was predicted to be the most likely site of autophosphorylation amongst the three sites within the same peptide identified by MALDI-MS (T313, T314, T316). In particular, the hydroxyl group of T316 is optimally oriented towards the proton acceptor residue in the TwcK active site (D277) and is ideally suited for modification *in cis*. Thus, residue T316 was selected for further mutational analysis, as described below. In addition, MS-based analysis of a purified, catalytically inactive TwcK^{K185A} protein sample revealed only the masses of the non-phosphorylated peptide for each of the pairs described above, permitting the phosphorylated peptides to be confidently attributed to auto-phosphorylation.

In summary, mass spectrometry studies revealed residues T212, T301, T401 or T412, and T316 as primary auto-phosphorylation sites in TwcK, with evidence for more infrequent S290 phosphorylation.

Analysis of phosphorylation sites by site-directed mutagenesis

The functional effect of auto-phosphorylation events was analysed by site-directed mutagenesis. TwcK mutants were constructed in which residues at each individual site were substituted for alanine: T212A, S234A, S290A, T301A, T316A, T401A, T412A. The mutants were expressed and purified, with the exception of $TwcK^{T401A}$, which yielded a completely insoluble protein product. Instead, a $TwcK^{T401D}$ mutant was generated at this site, which preserved the solubility of the kinase. All mutated samples were initially analysed by SDS-PAGE. $TwcK^{T212A}$ and $TwcK^{T316A}$ exhibited a marked difference in their electrophoretic profiles after SDS-PAGE (**Fig 3a**), apparently validating these two residues as phosphorylation sites.

A further analysis of TwcK phosphorylation site mutants using protease digestion and MALDI-MS measurements confirmed that peptides containing mutations T212A, T301A, T316A T401D lacked the phosphorylation site observed for wild-type TwcK, validating the loss of these possible phosphoacceptor sites. Notably, in TwcK samples carrying single mutations (T212A, T301A and T401D), non-mutated sites were still phosphorylated, proving that the mutated TwcK samples remained structurally viable and catalytically active. In contrast, the variant $TwcK^{T316A}$ showed no detectable phosphorylation at any site, suggesting that modification of this site silences catalysis and/or prevents an interaction with substrates.

TwcK auto-phosphorylation occurs in motifs mechanistically important for catalysis

To evaluate whether phosphorylation at the identified sites might have regulatory consequences on TwcK activity, we mapped the sites onto its crystal structure (PDB 3UTO) (**Fig 4**). The mapping revealed that three of the four sites (T212, T301, T316) were located in mechanistically important loci of the kinase fold, while the fourth site (T401) was remote from the active site. The positions of the individual residues were as follows:

i) T212 is located in the αC-β4 loop that immediately follows the catalytically relevant αC-helix. The loop commonly contains a conserved HxN motif that acts as hinge in the motions that take place when helix αC transitions between active and inactive conformations during catalysis. Accordingly, this motif is a known regulatory site in eukaryotic protein kinases (ePKs) and, although the His residue is conserved in some two thirds of the superfamily, it is replaced by a phosphorylatable Ser/Thr in ~10% of ePKs

(30,31). In *C. elegans* TwcK, the conserved asparagine of the HxN motif is replaced by T212, which interacts with H210 and H267, forming a polar-pi interaction with the latter. The phosphorylation of T212 could therefore alter the structural dynamics of this locus;

ii) T301 is located in the immediate vicinity of the conserved 297-DFG-299 motif. The aspartate residue in this motif coordinates the Mg^{2+} ion in the ATP/Mg^{2+} substrate and is essential for catalysis (32). It could be predicted that the introduction of a phosphate group at this position might negatively affect catalysis;

iii) T316 is in the P+1 loop of TwcK, facing directly into the active site towards the catalytic aspartate. The P+1 loop of protein kinases is critically involved in the binding of the peptidic substrate (26,33). Thus, the phosphorylation of residue T316 is likely to alter or even prevent substrate binding;

iv) T401 is not in close proximity of any known mechanistic element. Located at the bottom rear part of the C-terminal lobe of TwcK, T401 N-terminally caps the penultimate helix of the kinase fold. An equivalent phosphorylation site has been observed in ZIP kinase (34), but a function has not been attributed to this event. This region of the kinase fold has, however, been speculatively associated with protein-protein interactions based on the binding of PKA catalytic subunit to its regulatory subunit (35). It cannot be predicted at this time whether the modification of TwcK at site T401 has a functional consequence.

To assist our analysis of the possible effect of phosphorylation on TwcK, we estimated the energetics of the modification using FoldX (20). This software was used to calculate changes in the Gibbs free energy of folding (ΔΔG). Positive ΔΔG values are considered to be destabilizing to the protein fold and therefore likely to trigger structural aberrations, whereas negative ΔΔG values are considered stabilizing (20). Thus, ΔΔG values were calculated from *in silico* phosphorylated models based on the crystal structure of the TwcK catalytic domain (11) (**Fig 5a**). The values suggested that the phosphorylated side chains of residues T301 and T316 would be poorly accommodated in the fold and could therefore induce a conformational alteration. In particular, a visual inspection of the TwcK structure revealed that T301 is partly occluded within the kinase interlobular region, while T316 in the P+1 loop packs against the catalytic loop (**Fig 4**). To explore the structural consequences of these two modifications, we performed comparative molecular dynamics simulations (MDS) on the 3D-models of wild-type TwcK and its pT301 and pT316 variants (**Fig 5b,c**). Simulations (each carried out for a

total of 100 ns) suggested that the phosphoryl group of pT301 might be accommodated within the interlobular region of the fold with only minor rearrangements. It was therefore difficult to predict the impact of this site on catalysis. On the contrary, residue pT316 appeared to greatly increase the mobility of the P+1 loop with respect to the unphosphorylated state, possibly inducing disorder in this loop. Thereby, we concluded that the T316 site has a significant potential to disrupt the P+1 loop structurally. As even small changes to this region would have a large impact on the binding of the peptide substrate, we speculate that the phosphorylation of residue T316 might well contribute to the catalysis inhibition observed in the hyperphosphorylated states of TwcK.

Effect of phosphorylation on catalysis

To test our deductions, all mutants generated were assayed for phosphotransfer activity on a peptide model substrate (**Fig 3b).** In these assays, T212A and T316A substitutions showed the biggest effect on catalysis, displaying a pronounced reduction in activity to ~7% and <1% of the activity of wild-type TwcK, respectively. Next, the activity of two phosphomimetic substitutions, T212D and T316D, were measured. This revealed a recovery of activity in T212D (to ~70% of wild-type TwcK), while T316D exhibited a similarly low residual level of activity as observed for T316A. The loss of activity in T316A and T316D mutants confirms the critical mechanistic significance of the P+1 loop in TwcK. The result is reminiscent of a previous enzymatic analysis of the auto-phosphorylating kinase Mps1, in which mutation of the P+1 loop residue T686 to either alanine or aspartate completely abolished its activity *in vitro* and blocked its auto-phosphorylation function in cells (36-38).

In contrast, activity measurements demonstrated that substitutions T301A and T401D had little effect on TwcK catalytic activity towards the model peptide substrate, agreeing with our previously described analysis of TwcK auto-phosphorylation in SDS-PAGE; **Fig 3a**). This agrees with our predictions since alanine residues naturally occur in protein kinases at positions corresponding to T301 and T401 and these are surface-exposed residues with few structural constraints. In summary, our data suggest that phosphorylation at T316 is a primary modulator of TwcK catalytic output, while

additional sites of autophosphorylation might contribute cumulatively to the regulation of activity.

Discussion

Auto-phosphorylation is a common mechanism of kinase regulation. It often occurs within the kinase domain itself and it can lead to the activation of catalysis through the rearrangement of the active site into a productive state (39,40). In titin-like kinases, the catalytically relevant groups already adopt an active conformation and appear primed for productive substrate binding and phosphotransfer (5,41). Thus, regulation by auto-phosphorylation was not anticipated to be involved in their catalytic regulation. In contrast to this expectation, we have found that TwcK undergoes auto-phosphorylation at mechanistically important loci: in the αC-β4 loop (T212); immediately adjacent to the DFG motif at the beginning of the activation segment (T301) and in the P+1 loop, at the end of the activation segment (T316). We show that, in net terms, auto-phosphorylation decreases or even abolishes catalysis in TwcK. Of the phosphorylation sites identified in this study (T212, T301, T316 and T401), the modification of residue T316 in the P+1 loop appears to be a key event, with the disruption of activity in both $TwcK^{T316A}$ and $TwcK^{T316D}$ mutants predictably being a consequence of reduced affinity for the peptide substrate, which interacts with this region in canonical protein kinases.

Modulation of catalytic activity by phosphorylation in the P+1 loop has been observed in several other kinases. For example, in Mps1, auto-phosphorylation at a P+1 loop residue (T686) is associated with catalytic activity (37). Complete dephosphorylation and inactivation of Mps1 is followed by rapid reactivation upon ATP exposure, whereas mutation of the T686 P+1 residue to either alanine or aspartate completely abolishes activity and reactivation (37). In contrast, phosphorylation of the equivalent residue (T180) in Zipper Interacting Protein Kinase (ZIPK), a member of the DAPK family, abolishes its catalytic activity (34). Comparable cases are the phosphorylation of Plk1 (Y217) and Plk4 (Y170) at a conserved tyrosine residue in the P+1 loop that has recently been proposed to inhibit the activity of these kinases by up-stream tyrosine kinases (42,43). Similarly, microtubule affinity regulating kinase 2 (MARK2) becomes totally inactivated when phosphorylated by MARKK at S212 in the

P+1 loop (44). Interestingly, in these kinases (Mps1, ZIPK and MARK2) mutation of the phosphorylatable residue to either aspartate/glutamate or alanine abolished kinase activity, independently of whether the phosphorylation event itself was activating or inactivating. This demonstrates the high sensitivity of this locus to modification and the difficulty of concluding on the regulatory role of a given phosphorylation event on kinases. In addition to these cases of positive and negative regulation, P+1 loop phosphorylation has also been reported to change substrate specificity in the mitotic kinase Bub1 (45). Crystal structures of both the P+1 unphosphorylated (PDB: 4R8Q) and P+1 phosphorylated forms (PDB: 4QPM) confirm that phosphorylation at S969 forces the loop out from the active site and changes its conformation. This change in Bub1 enables discrimination between two *in vivo* substrates, H2A and cdc20. Phosphorylation at S969 greatly increased H2A phosphorylation but had no effect on cdc20, indicating that the rearrangement of the P+1 loop upon phosphorylation influenced substrate specificity (45). Our current data on TwcK appear to indicate that the phosphorylation of T316 is the deterministic inhibitory event, with the modification of other residues possibly having a cumulative effect. However, we cannot discard the possibility that the T316D mutant does not mimic well the phosphorylated state and, instead, low catalysis is due to a locally compromised catalytic region in the kinase. Concluding unambiguously on the role of the T316 site in TwcK will require future mechanistic and kinetic studies.

An analysis of sequence conservation (sequence alignments in 5,11) suggests that similar phosphorylation events could occur in other members of the titin-like kinase family. Of the sites identified in this study, sites T401 and T316 recur across the family and, if substituted, are often replaced by other phosphorylatable residues. Specifically, the equivalent residue to T401 is the most conserved site in the family. It is present in all TwcKs (where it is strictly conserved), in vertebrate titin kinases, in vertebrate obscurin PK1 kinases (where it is commonly a Ser residue) and in the invertebrate homolog UNC-89 PK1 kinases. Interestingly, in UNC-89 PK1 kinases from insects, this residue is commonly an aspartate, suggesting that in that animal group this locus could mimic the permanently phosphorylated state. In UNC-89 PK2 kinases from insects this residue is often a tyrosine, possibly pointing to the action of an up-stream kinase. While its high conservation might indicate that T401 is an important regulatory site, the functional role of this locus (which maps to the bottom-rear part of the kinase fold and distant from catalytically relevant regions) is unknown. Interestingly, phosphorylation at an equivalent

site has been also observed in ZIPK of the DAPK family (34), a kinase family closely related to titin-like kinases (41). Currently, it is suspected that this region of the kinase fold supports interactions with other cellular proteins (35). The second conserved phosphorylation site is T316 in the P+1 loop, which is present either as a Ser or Thr across TwcKs, obscurin and UNC-89 PK1 kinases. Although other members of the family also harbour phosphorylatable residues in the P+1 loop, the loop has a variable structure in kinases and we could not conclude reliably on the conservation of this site in other family members. Interestingly, and similar to many AGC and Polo-like kinases, human titin kinase (TK) contains phosphorylatable tyrosine residues in this loop, which have been proposed to undergo phosphorylation based on the use of anti-phosphotyrosine antibodies (14,16). However, a more recent MS analysis of wild-type and YtoE TK samples expressed in eukaryotic cells failed to detect any phosphorylated sites (6). Further studies will be required to conclusively resolve this issue for TK. The predicted importance of tyrosine phosphorylation in this loop for the regulation of multiple Ser/Thr kinases (42,43) makes this an important future goal. In summary, our findings suggest a likely overall significance to the titin-kinase family of phosphorylation at T401 and T316 equivalent locations.

In addition to a role in catalysis, phosphorylation might also regulate the scaffolding interactions of titin-like kinases with their cellular partners, which are often signalling proteins as kinases, phosphatases and protein turn-over factors. In TwcK, MAPKAP kinase 2 (MAK-1) was shown to interact with and phosphorylate its CRD tail (8). *D. melanogaster* UNC-89 PK1 interacts with MASK kinase (46) and *C.elegans* UNC-89 PK1 and PK2 kinases interact with the SCPL-1 phosphatase (47). TK binds the autophagy receptors nbr1 and p62 (7) and the E3 ubiquitin ligases MuRF1 (6) and MuRF2 (7). It is interesting to note that various members of the titin-like kinase family, including UNC-89 PK1 and human TK, have been suggested to be pseudokinases with no or very low activity (5,6,27). It is conceivable that these pseudokinases might be subject to phosphorylation by up-stream kinases that regulate their scaffolding interactions.

Inhibition by autophosphorylation adds to the established dual intrasteric blockage of TwcK by N- and C-terminal tails, resulting in a triple auto-inhibitory mechanism, suggesting that the activity of this kinase must be tightly regulated *in vivo*. The results also suggest that the control of TwcK activity not only involves mechanical

processes but also biochemical regulation (**Fig 6**). In this respect, diverse molecular species were observed by SDS-PAGE for an NL-TwcK construct containing the single regulatory extension NL, whereas only a single species (that was not affected by phosphatase treatment) was observed for the fully autoinhibited TwcK containing both NL and CRD extensions (NL-Kin-CRD) (**Fig 3a)**. This indicates that the partially autoinhibited NL-TwcK is able to undergo auto-phosphorylation whereas fully inhibited TwcK is not. It can be concluded that auto-phosphorylation can occur in mechanically activated states of TwcK, which could turn inactive in this way. This implies that mechanically stretched conformations of TwcK do not necessarily correspond to catalytically active states. In turn, phosphorylation might further inhibit the repacking of the tails against the kinase domain once the mechanical stimulus has ceased, extending the lifetime of the stretch-induced conformation beyond the presence of the mechanical cue that triggered it. Thereby, phosphorylation could decouple to some extent mechanical cues from TwcK catalytic response. The recovery of catalytic activity would require the action of a specific phosphatase. To investigate this possibility, we tested the activity of SCPL-1 towards phosphorylated TwcK. SCPL-1 is a CTD-type protein phosphatase of *C. elegans* body wall muscle that is known to interact with the titin-like PK1 and PK2 kinases of UNC-89 (47). However, SCPL-1 did not elicit any change in the SDS-PAGE banding pattern of recombinant TwcK, so that a possible physiological phosphatase cannot be proposed at this time. All considered, this model of TwcK regulation (**Fig 6**) might imply that TwcK is in a largely inhibited state *in vivo*, at least on muscle under sustained strain. In this respect, a recent study has explored the impact of TwcK catalysis in *C. elegans in vivo* (28). In that work, CRISPR/Cas9 gene editing was used to create nematodes that expressed twitchin containing the inactive TwcK^{K185A} variant (only). The mutated worms displayed structurally-intact sarcomeres. However, they moved faster than wild-type worms and their muscles contracted more. The data suggested that the catalytic activity of TwcK inhibits muscle activity. Yet the phenotype of the TwcK^{K185A} mutant worms was very mild. The findings of our current study lead us now to consider whether TwcK might exhibit only low levels of activity in the sarcomere. Future studies on TwcK and titin-like kinases are, therefore, required to elucidate the relative functional significance of catalysis versus scaffolding in these sarcoskeletal kinases.

Author contribution

OM conceived and coordinated the study. OM and RW wrote the paper. RW and BF performed all molecular biology, biochemical and catalytic work. MW performed MS studies. PAE assisted with catalytic analyses. JF and DJR performed and evaluated MDS. GMB provided technical and scientific assistance. All authors reviewed the results, edited the manuscript and approved the final version of the manuscript.

Acknowledgements

We acknowledge funding from HFSP (RGP0044/2012) and a BBSRC-DTP studentship to RW. PAE acknowledges funding from BBSRC grant BB/N021703. We thank the Proteomics Facility at the University of Konstanz for mass spectrometric analysis.

Conflicts of interest

The authors declare that they have no conflicts of interest with the contents of this article.

FIGURE LEGENDS

Figure 1: Recombinant TwcK samples are phosphorylated

Recombinant, purified TwcK consists of multiple electrophoretic species that are poorly resolved by chromatography; **a.** Size exclusion chromatogram (SEC) of TwcK and its corresponding SDS-PAGE. Numbered fractions are those assayed for activity in c.; **b.** SDS-PAGE analysis of TwcK before and after treatment with λ-phosphatase showing the collapse of multiple species into a single band of molecular mass similar to that of the inactive mutant $TwcK^{K185A}$. Numbering denotes the molecular mass (kDa) of marker proteins; **c.** Measurement of phosphotransfer catalysis by TwcK samples on a model peptide substrate monitored using [γ^{32}P]-ATP. Hyper- [SEC fraction 1] and hypo- [SEC fraction 3] phosphorylated states and a mixture containing roughly an equal proportion of both states [SEC fraction 2] analysed by SDS-PAGE in a. Coomassie staining was used for all SDS-PAGE shown.

Figure 2: Analysis of TwcK phosphorylation by mass spectrometry

ES-MS intact mass spectra for (**a**) TwcK and (**b**) TwcK after λ-phosphatase treatment. Untreated TwcK is a mixture of species differing by the mass of a phosphoryl group or

multiples thereof. All major species observed by ES-MS for untreated TwcK are of a higher molecular mass than that of unmodified TwcK calculated from sequence data. Following λ-phosphatase treatment, TwcK ES-MS spectra consist of one major species corresponding to the unmodified TwcK. The observed peak at 32615.0 Da corresponds to the $[M+Na^+]$ ion for dephosphorylated TwcK, with minor peaks of higher mass likely due to incomplete dephosphorylation of TwcK by the phosphatase; **c.** MALDI-MS spectra following tryptic digest of TwcK and phosphopeptide enrichment.

Figure 3: Catalysis by TwcK phosphorylation site mutants

a. SDS-PAGE analysis of TwcK phosphorylation site mutants; **b.** Activity of TwcK phosphor-mutants towards a model peptide substrate measured using [□32P] ATP. The various wild-type TwcK states are shown as reference. Hyper-P refers to the predominant species contributing to the 'upper bands' of SDS-PAGE (i.e. molecular species with less electrophoretic mobility) and corresponding to higher phosphorylation states. Hypo-P samples mainly consist of species from 'lower bands' in SDS-PAGE (i.e. higher electrophoretic mobility), corresponding to reduced levels of autophosphorylation. Values (as %) are relative to the activity of lambda-phosphatase treated TwcK.

Figure 4: Location of phosphorylation sites in the TwcK molecule

Identified auto-phosphorylation sites are mapped onto the crystal structure of the catalytic domain of TwcK (extracted from PDB 3UTO). Catalytically important regions of the kinase fold are highlighted.

Figure 5: Computational assessment of phosphorylation effects

a. FoldX evaluation of structural tolerance to phosphorylation at the identified sites; **b.** Putty cartoon representation of the different backbone structures with the relative root-mean-squared fluctuation of residues through the simulation represented by color and line thickness: red and thick, more movement; blue and thin, less movement. Phosphorylation sites are shown as cyan sticks; **c.** Relative fluctuation plotted against residue. Wildtype, orange; green, pT212; cyan pT301; dark blue, pT316. Units are arbitrary.

Figure 6: Predicted mechano-biochemical cycle of TwcK regulation

In its ground state, TwcK is inhibited by two N- and C-terminal tail extensions, termed NL and CRD, that pack against the kinase domain blocking the active site and the kinase hinge region (NL: yellow; CRD: red; kinase: grey surface representation; (11)). The tails are displaced from the kinase active site by the mechanical stretch that develops in the sarcoskeleton during muscle function. Mechanically-activated states of TwcK could turn inactive by autophosphorylation. Reverting TwcK to its conformational and catalytic ground state must require the intervention of a phosphatase.

References

1. Krüger, M., Linke, W.A. (2011) The giant protein titin: a regulatory node that integrates myocyte signaling pathways. *J. Biol. Chem.* **286**, 9905-9912
2. Gieseler, K., Qadota, H., Benian, G.M. (April 13, 2017) Development, structure, and maintenance of *C. elegans* body wall muscle. *WormBook*, ed. The *C. elegans* Research Community, WormBook, doi/10.1895/wormbook.1.81.2, http://www.wormbook.org
3. Bullard, B., Linke, W., Leonard, K. (2002) Varieties of elastic protein in invertebrate muscles. *J. Muscle. Res. Cell. Motil.* **23**, 435-447
4. Kontrogianni-Konstantopoulos, A., Ackerman, M.A., Bowman, A.L., Yap, S.V., Bloch, R.J. (2009) Muscle giants: Molecular scaffolds in sarcomerogenesis. *Physiol. Rev.* **89**, 1217-1267
5. Mayans, O., Benian, G.M., Simkovic, F., Rigden, D.J. (2013) Mechanistic and functional diversity in the mechanosensory kinases of the titin-like family. *Biochem. Soc. Trans.* **41**, 1066-1071
6. Bogomolovas, J., Gasch, A., Simkovic, F., Rigden, D.J., Labeit, S., Mayans, O. (2014) Titin kinase is an inactive pseudokinase scaffold that supports MuRF1 recruitment to the sarcomeric M-line. *Open Biol.* **4**, 140041
7. Lange, S., Xiang, F., Yakovenko, A., Vihola, A., Hackman, P., Rostkova, E., Kristensen, J., Brandmeier, B., Franzen, G., Hedberg, B., Gunnarsson, L.G., Hughes, S.M., Marchand, S., Sejersen, T., Richard, I., Edström, L., Ehler, E., Udd, B., Gautel, M. (2005). The kinase domain of titin controls muscle gene expression and protein turnover. *Science* **308**, 1599-603.
8. Matsunaga, Y., Qatoda, H., Furukawa, M., Choe, H.H., Benian, G.M. (2015) Twitchin kinase interacts with MAPKAP kinase 2 in *Caenorhabditis elegans* striated muscle. *Mol. Biol. Cell.* **26**, 2096-2111
9. Hu, S.H., Parker, M.W., Lei, J.Y., Wilce, M.C., Benian, G.M., Kemp, B.E. (1994) Insights into autoregulation from the crystal structure of twitchin kinase. *Nature* **369**, 581-585
10. Kobe, B., Heierhorst, J., Feil, S.C., Parker, M.W., Benian, G.M., Weiss, K.R., Kemp, B.E. (1996) Giant protein kinases: domain interactions and structural basis of autoregulation. *EMBO J.* **15**, 6810-6821
11. von Castelmur, E., Strumpfer, J., Franke, B., Bogomolovas, J., Barbieri, S., Qatoda, H., Konarev, P.V., Svergun, D.I., Labeit, S., Benian, G.M., Schultein, K., Mayans, O. (2012) Identification of an N-terminal inhibitory extension as the primary mechanosensory regulator of twitchin kinase. *Proc. Natl. Acad. Sci. U.S.A.* **109**, 13608-13613
12. Lei, J., Tang, X., Chambers, T.C., Pohl, J., Benian, G.M. (1994). Protein kinase domain of twitchin has protein kinase actvitiy and an autoinhibitory region. *J. Biol. Chem.* **269**, 21078-21085
13. Heierhorst, J., Tang, X., Lei, J., Probst, W.C., Weiss, K.R., Kemp, B.E., Benian, G.M. (1996) Substrate specificity and inhibitor sensitivity of Ca^{2+}/S-100-dependent twitchin kinases. *Eur. J. Biochem.* **242**, 454-459
14. Mayans, O., van der Ven, P.F., Wilm, M., Mues, A., Young, P., Fürst, D.O., Wilmanns, M., Gautel, M. (1998) Structural basis for activation of the titin kinase domain during myofibrillogenesis. *Nature* **395**, 863-869
15. Gräter, F., Shen, J., Jiang, H., Gautel, M., Grubmüller, H. (2005) Mechanically induced titin-kinase activation studied by force-probe molecular dynamics simulations. *Biophys. J.* **88**, 790-804

16. Puchner, E.M., Alexandrovich, A., Kho, A.L., Hensen, U., Schäfer, L.V., Brandmeier, B., Gräter, F., Grubmüller, H., Gaub, H.E., Gautel, M. (2008) Mechanoenzymatics of titin kinase. *Proc. Natl. Acad. Sci. U.S.A.* **105**, 13385-13390
17. Greene, D.N., Garcia, T., Sutton, R.B., Gernert, K.M., Benian, G.M., Oberhauser, A.F. (2008) Single-molecular force spectroscopy reveals a stepwise unfolding of Caenorhabditis elegans giant protein kinase domains. *Biophys. J.* **95**, 1360-1370
18. Heierhorst, J., Probst, W.C., Vilim, F.S., Buku, A., Weiss, K.R. (1994) Autophosphorylation of molluscan twitchin and interaction of its kinase domain with calcium/calmodulin. *J. Biol. Chem.* **269**, 21086-21093
19. Bem, E.M., Bem, H., Reimchüssel, W. (1980) Determination of phosphorus-32 and calcium-45 in biological samples by Cerenkov and liquid scintillation counting. *Appl. Radiat.Isot.* **31**, 371-374
20. Schymkowitz, J., Borg, J., Stricher, F., Nys, R., Rousseau, F., Serrano, L. (2005) The FoldX web server: an online force field. *Nucleic Acids Res.* **33**, W382-W388
21. Margreitter, C., Petrov, D., Zagrovic, B. (2013) Vienna-PTM webserver: a toolkit for MD simulations of protein post-translational modifications. *Nucleic Acids Res.* **41,** W422-426
22. Van Der Spoel, D., Lindahl, E., Hess, B., Groenhof, G., Mark, A.E., Berendsen, H.J. (2005) GROMACS: fast, flexible, and free. *J. Comput. Chem.* 26, 1701-1718.
23. Lindorff-Larsen, K., Piana, S., Palmo, K., Maragakis, P., Klepeis, J.L., Dror, R.O., Shaw, D.E. (2010) Improved side-chain torsion potentials for the Amber ff99SB protein force field. *Proteins* **78**, 1950-1958
24. Darden, T., Perera, L., Li, L., Pedersen, L. (1999) New tricks for modelers from the crystallography toolkit: the particle mesh Ewald algorithm and its use in nucleic acid simulations. *Structure* **7**, R55-60
25. Berk, H., Bekker, H., Berendsen, H.J.C., Fraaije, J.G.E.M. (1997) LINCS: a linear constraint solver for molecular simulations. *J. Comp. Chem.* **18**, 1463-1472
26. Endicott, J.A., Noble, M.E.M., Johnson, L.N. (2012) The structural basis for control of eukaryotic protein kinases. *Annu. Rev. Biochem.* **81**, 587-613
27. Reiterer, V., Eyers, P.A., Farhan, H. (2014) Day of the dead: pseudokinases and pseudophosphatases in physiology and disease. *Trends Cell Biol.* **24**, 489-505
28. Cross, D.A., Alessi, D.R., Cohen, P., Andjelkovich, N., Hemmings, B.A. (1995) Inhibition of glycogen synthase kinase-3 by insulin mediated by protein kinase B. *Nature* **378**, 785-789
29. Kannan, N., Neuwald, A.F. (2005) Did protein kinase regulatory mechanisms evolve through elaboration of a simple structural component? *J. Mol. Biol.* **351**, 956-972
30. Kannan, N., Neuwald., Taylor, S.S. (2007) Analogous regulatory sites within the αC-β4 loop regions of ZAP-70 tyrosine kinase and AGC kinases. *Biochim. Biophys. Acta.* **1784**, 27-32.
31. Knighton, D. R., Zheng, J. H., Eyck, Ten, L. F., Xuong, N. H., Taylor, S. S., Sowadski, J. M. (1991) Structure of a peptide inhibitor bound to the catalytic subunit of cyclic adenosine monophosphate-dependent protein kinase. *Science* **253**, 414–420.
32. Johnson, L.N., Lewis, R.J. (2001) Structural basis for control by phosphorylation. *Chem. Rev.* **101**, 2209-2242
33. Graves, P.R., Winkfield, K.M., Haystead, T.A.J. (2005) Regulation of zipper-interacting protein kinase activity *in vitro* and *in vivo* by multisite phosphorylation. *J. Biol. Chem.* **280**, 9363-9374

34. McClendon, C.L., Kornev, A.P., Gilson, M.K., Taylor, S.S. (2014) Dynamic architecture of a protein kinase. *Proc Natl Acad Sci U.S.A.* **111**, 4623-4631
35. Chu, M.L., Chavas, L.M., Douglas, K.T., Eyers, P.A., Tabernero, L. (2008) Crystal structure of the catalytic domain of the mitotic checkpoint kinase Mps1 in complex with SP600125. *J. Biol. Chem.* **282**, 21495-21500
36. Tyler, R.K., Chu, M.L., Johnson, H., McKenzie, E.A., Gaskell, S.J., Eyers, P.A. (2009) Phosphoregulation of human Mps1 kinase. *Biochem. J.* **417**, 173-181
37. Chu, M.L., Lang, Z., Chavas, L.M., Neres, J., Fedorova, O.S., Tabernero, L., Cherry, M., Williams, D.H., Douglas, K.T., Eyers, P.A. (2010) Biophysical and X-ray crystallographic analysis of Mps1 kinase inhibitor complexes. *Biochemistry* **49**, 1689-1701
38. Nolen, B., Ngo, J., Chakrabarti, S., Vu, D., Adams, J.A., Ghosh, G. (2003) Nucleotide-induced conformational changes in the Saccharomyces cerevisiae SR protein kinase, Sky1p, revealed by X-ray crystallography. *Biochemistry* **42**, 9575-9585
39. Steichen, J.M., Kuchinskas, M., Keshwani, M.M., Yang, J., Adams, J.A., Taylor, S.S. (2012) Structural basis for the regulation of protein kinase A by activation loop phosphorylation. *J. Biol. Chem.* **287**, 14672-14680
40. Temmerman, K., Simon, B., Wilmanns, M. (2013). Structural and functional diversity in the activity and regulation of DAPK-related protein kinases. *FEBS J.* **280**, 5533-50.
41. Caron, D., Byrne, D.P., Thebault, P., Soulet, D., Landry, C.R., Eyers, P.A., Elowe, S. (2016) Mitotic phosphotyrosine network analysis reveals that tyrosine phosphorylation regulates Polo-like kinase 1 (PLK1). *Sci. Signal.* **9**, rs14
42. McSkimming, D.I., Dastgheib, S., Baffi, T.R., Byrne, D.P., Ferries, S., Scott, S.T., Newton, A.C., Eyers, C.E., Kochut, K.J., Eyers, P.A., Kannan, N. (2016) KinView: a visual comparative sequence analysis tool for integrated kinome research. *Mol. Biosyst* **12**, 3651-3665
43. Timm, T., Li, X.Y., Biernat, J., Jiao, J., Mandelkow, E., Vandekerckhove, J., Mandelkow, E.M. (2003) MARKK, a Ste20-like kinase, activates the polarity-inducing kinase MARK-PAR-1. *EMBO J.* **22**, 5090-5101
44. Lin, Z., Jia, L., Tomchick, D.R., Luo, X., Yu, H. (2014) Substrate-specific activation of the mitotic kinase Bub1 through intramolecular autophosphorylation and kinetochore targeting. *Structure* **22**, 1616-1627
45. Katzemich, A., West, R.J., Fukuzawa, A., Sweeney, S.T., Gautel, M., Sparrow, J., Bullard, B. (2015) Binding partners of the kinase domains in Drosophila obscurin and their effect on the structure of the flight muscle. *J. Cell Sci.* **128**, 3386-3397
46. Qadota, H., McGaha, L.A., Mercer, K.B., Stark, T.J., Ferrara, T.M., Benian, G.M. (2008) A novel protein phosphatase is a binding partner for the protein kinase domains of UNC-89 (obscurin) in Caenorhabditis elegans. *Mol. Biol. Cell* **19**, 2424-2432
47. Small, T.M., Gernert, K.M., Flaherty, D.B., Mercer, K.B., Borodovsky, M., Benian, G.M. (2004). Three new isoforms of *Caenorhabditis elegans* UNC-89 containing MLCK-like protein kinase domains. *J. Mol. Biol.* **342**, 91-108
48. Matsunaga, Y., Hwang, H., Franke, B., Williams, R., Penley, M., Qadota, H., Yi, H., Morran, L.T., Lu, H., Mayans, O., Benian, G.M. (2017). Twitchin kinase inhibits muscle activity. *Mol. Biol. Cell.* **28**, 1591-1600.

Figure 1

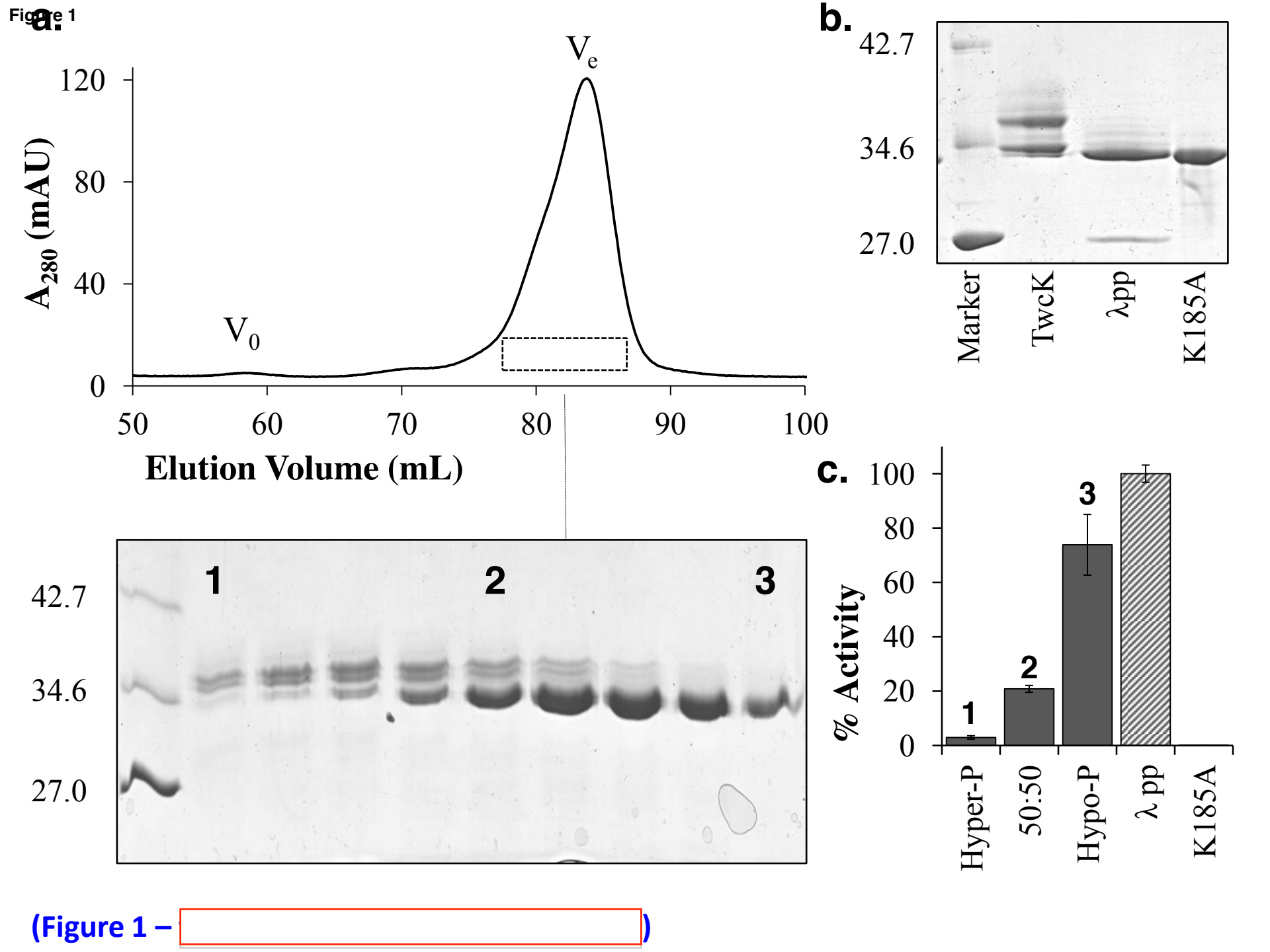

(Figure 1 –)

Figure 2

(Fig 2)

a. TwcK intact mass

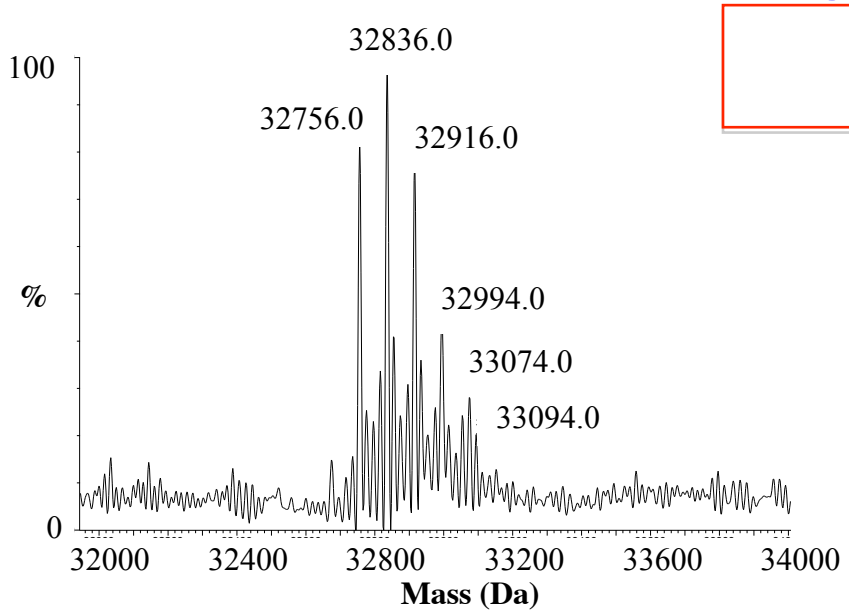

b. TwcK phosphatase treated intact mass

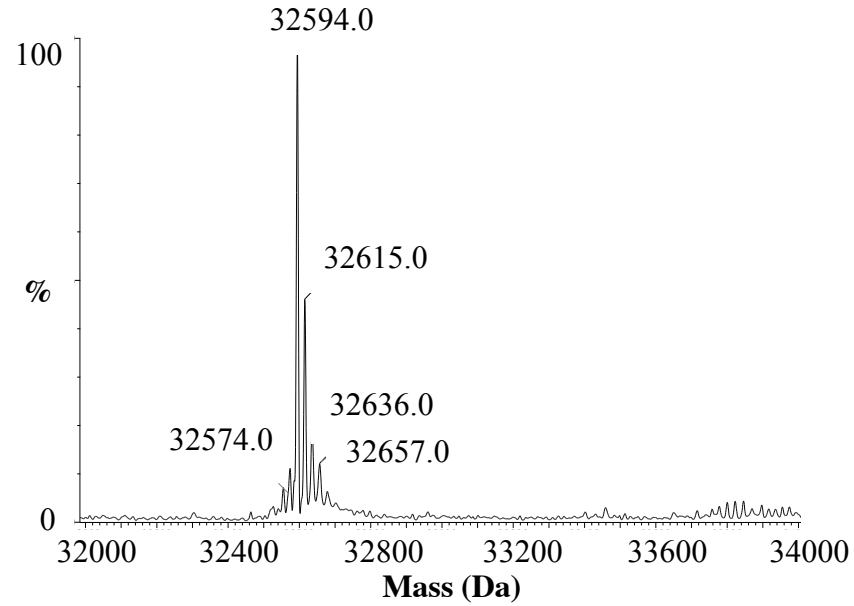

c. TwcK trypsin digested

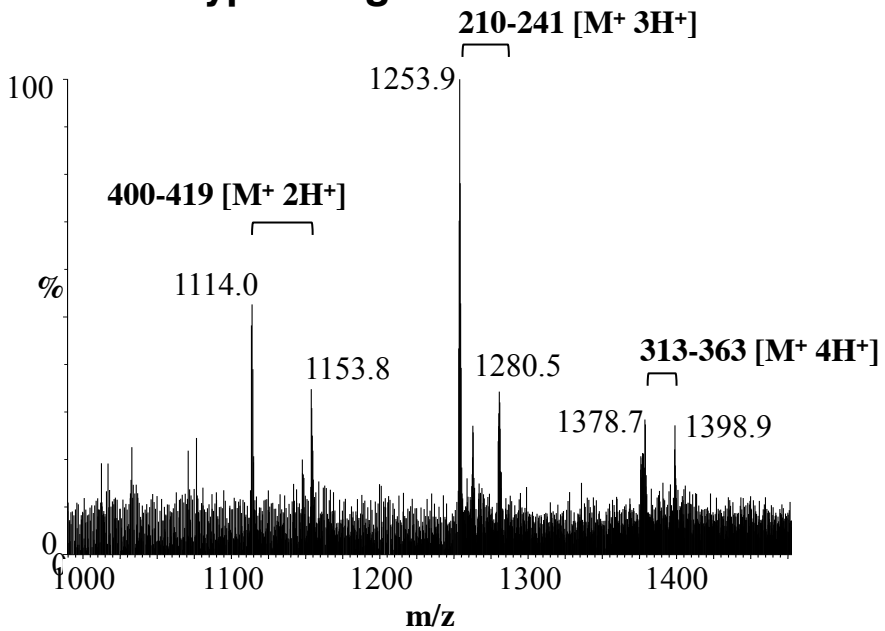

Figure 3

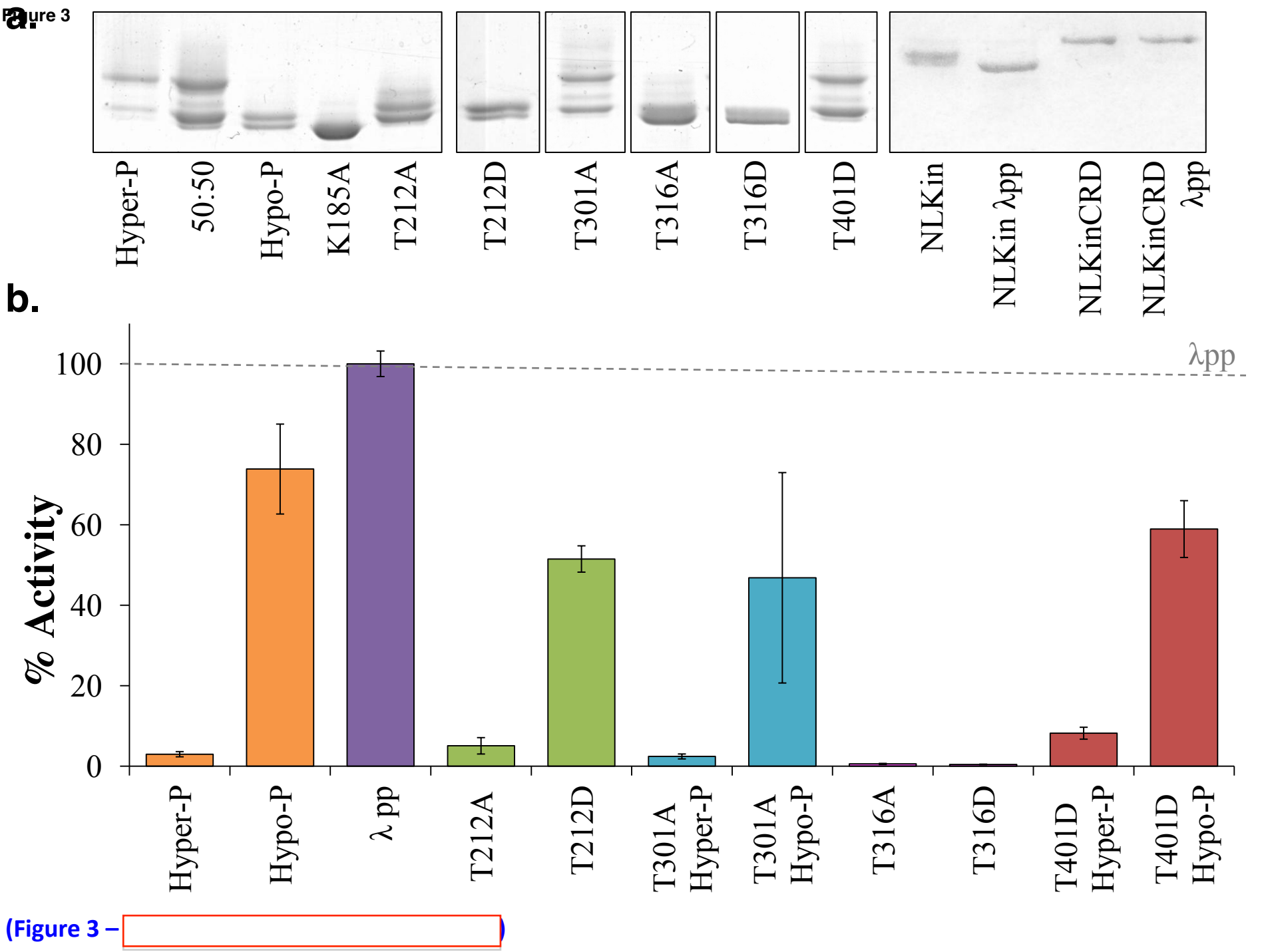

(Figure 3 –

Figure 4

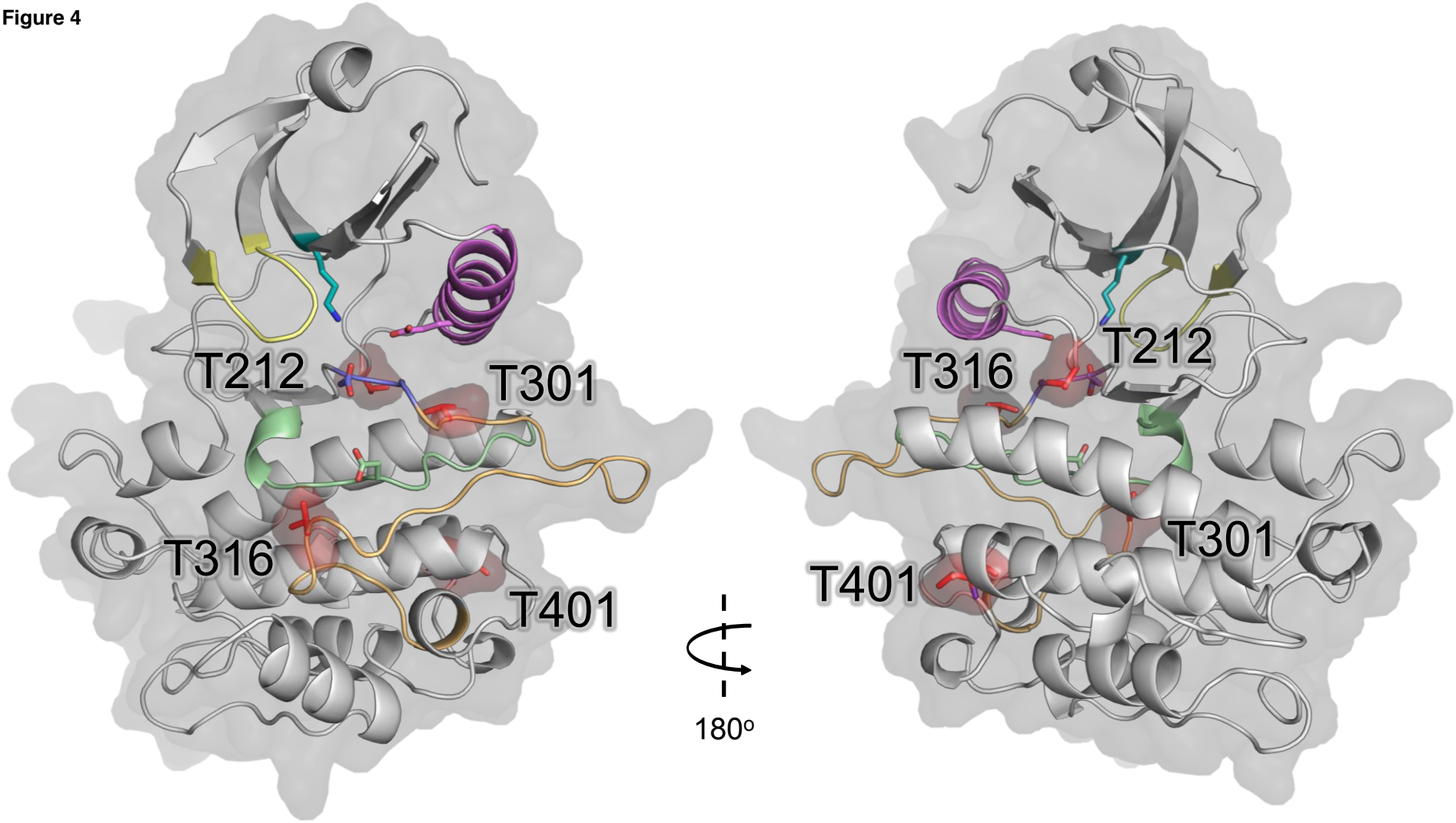

GxGxxG β3 lysine αC-helix Catalytic loop DFG

Activation segment Phosphorylation site

(Figure 4 –)

Figure 5a

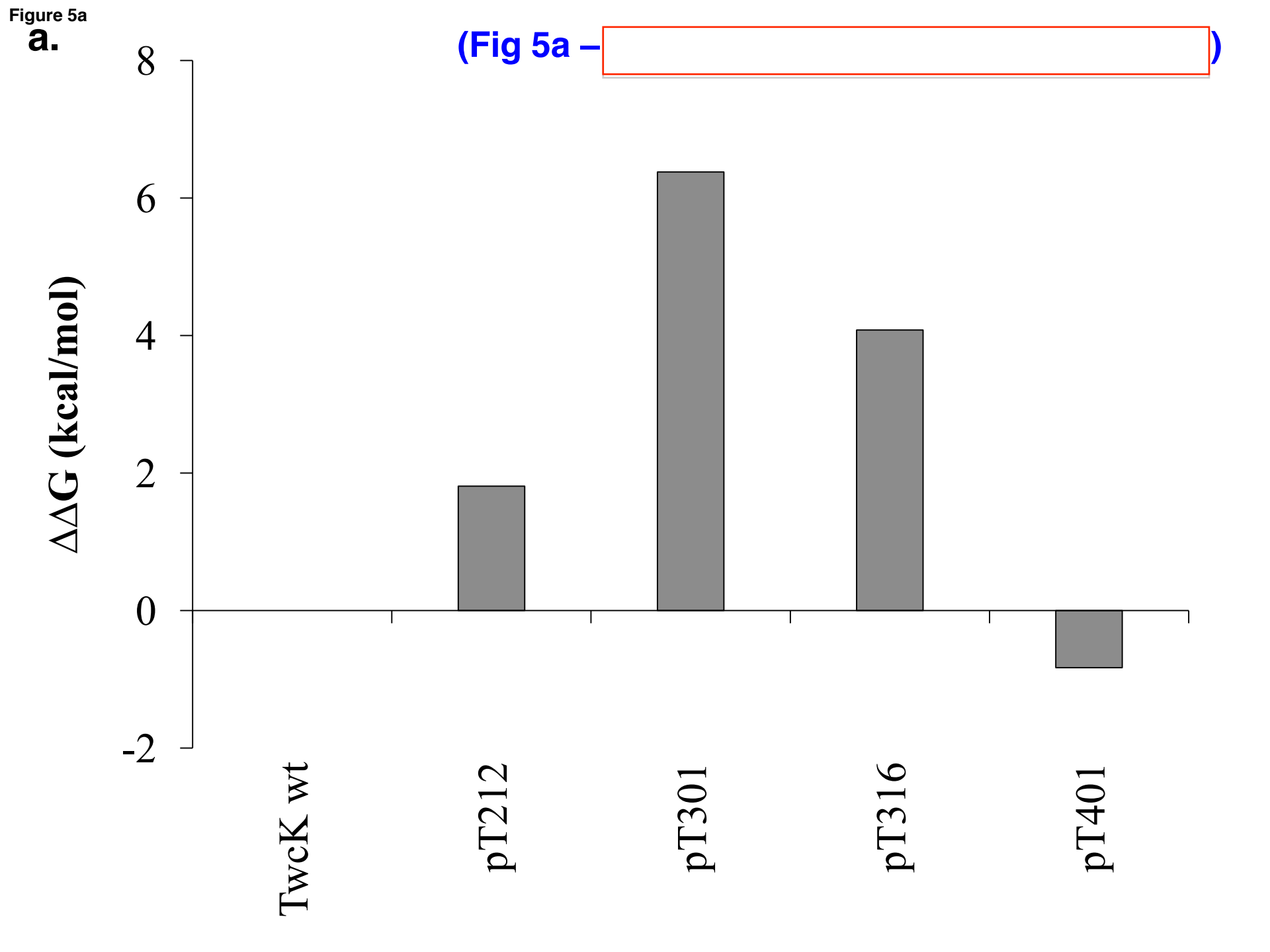

Figure 5bc

b.

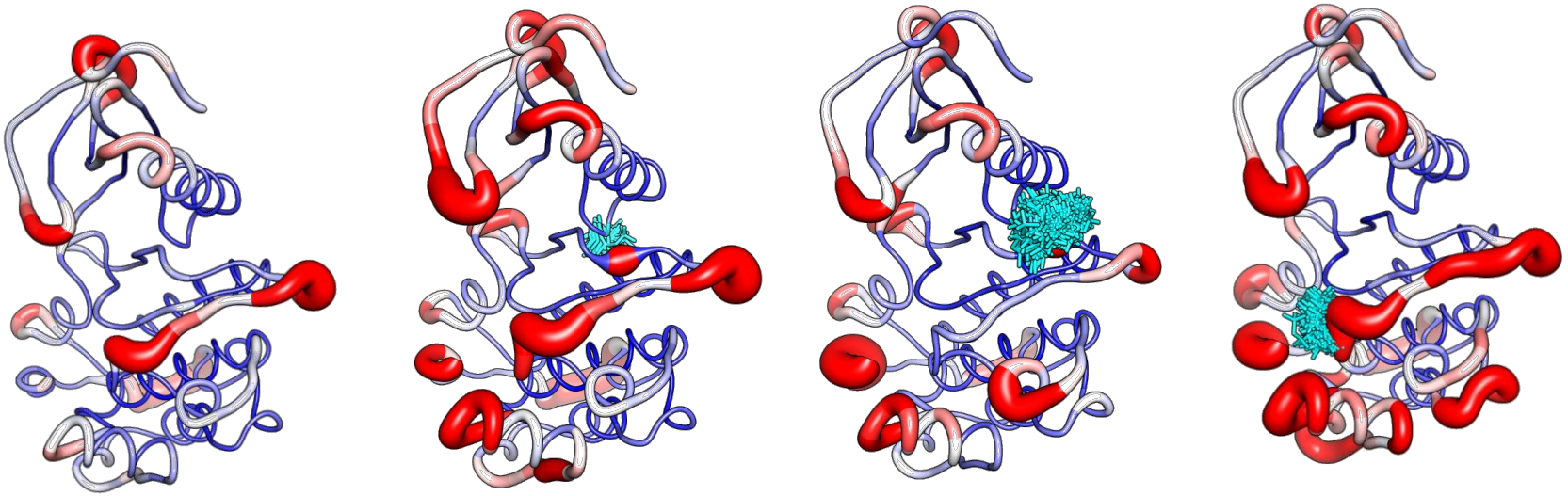

c.

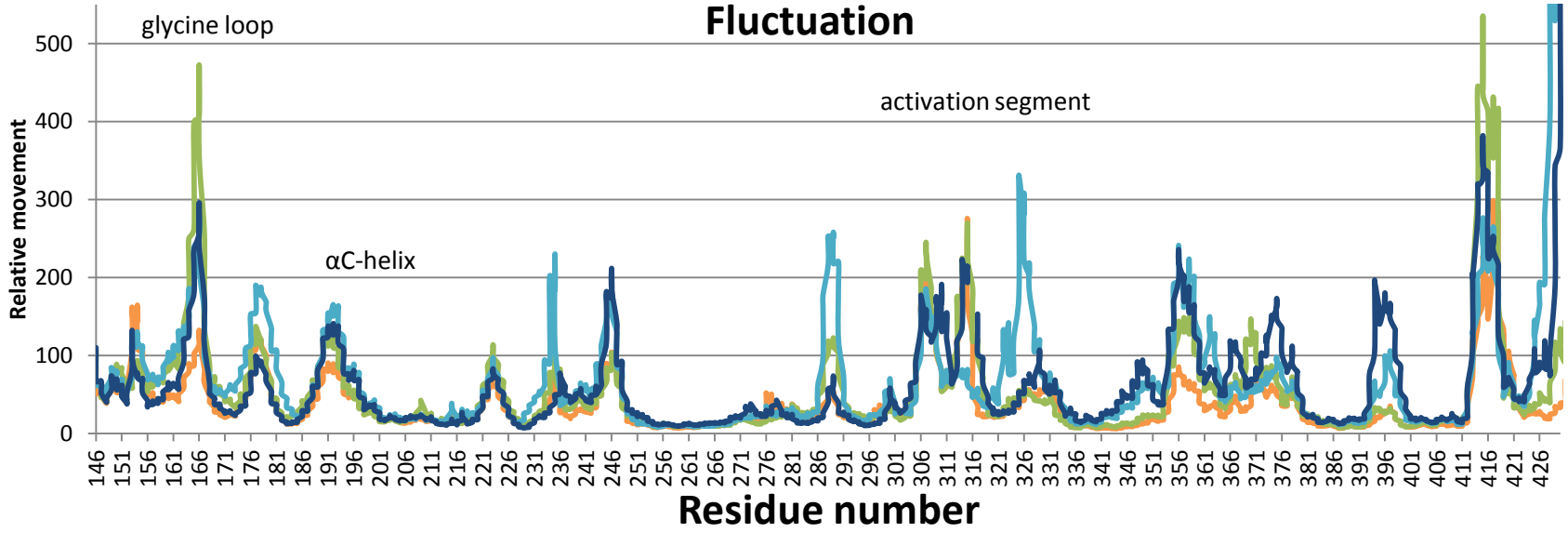

(Fig 5 -

Figure 6

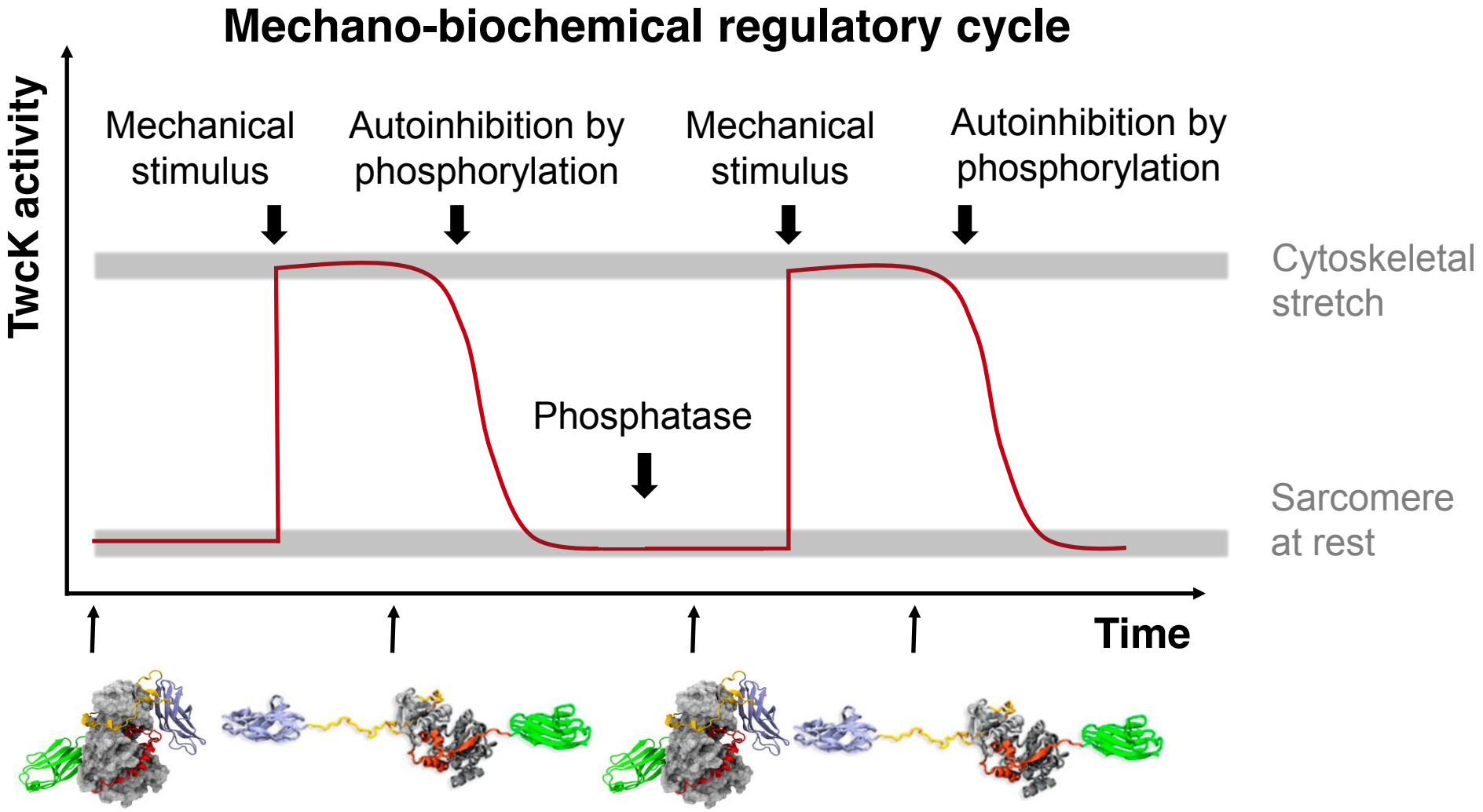

(Figure 6 –)